NASA IRTF / UNIVERSITY OF HAWAII

Document #: RQD-1.3.3.7-01-X.doc

Created on : Oct 15/10
Last Modified on : Oct 15/10

SCIENCE CASE

Authors: John Rayner and the iSHELL science team

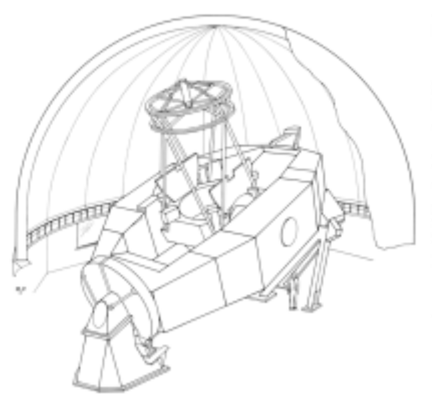

NASA Infrared Telescope Facility
Institute for Astronomy
University of Hawaii

Revision History

Revision No.	Author & Date	Approval & Date	Description
Revision 1	John Rayner 2/8/13		Preliminary Release.

Contents

1 Introduction

iSHELL is planned as a replacement for CSHELL, which had first light in 1993. CSHELL is a single-order echelle spectrograph and uses a single 256x256 InSb array. CSHELL is one of only a few high-resolution 1-5 µm echelle spectrographs available to observers in the northern hemisphere. Despite its age and small simultaneous wavelength range (about 0.006 µm at 2.2 µm) CSHELL still averages about 15% of IRTF telescope time. Capitalizing on technological developments in spectrograph gratings and infrared arrays iSHELL will provide greatly improved capabilities over CSHELL. The use of a Teledyne 2048x2048 Hawaii 2RG (H2RG) in the spectrograph combined with a cross-dispersed spectral format will increase the simultaneous wavelength coverage by about 20-100 times depending on selected slit length. Also, by employing silicon immersion gratings to reduce the required collimated beam diameter, the resolving power will be doubled to R=70,000 while at the same time keeping the cryostat relatively compact.

2. Science Case

As an IRTF facility instrument iSHELL needs to fulfill the needs of a diverse community of users for over a decade of service. iSHELL is therefore designed to be as flexible as time and budget allows. A number of key science cases have been explored by the Science Team to develop instrument design drivers, although many other science programs are enabled. The members of the Science Team are:

- Allende-Prieto (U. of Texas)
- G. Bjoraker (Goddard Space Flight Center)
- J. Carr (Naval Research Lab)
- N. Dello Russo (Johns Hopkins/APL)
- D. Deming (GSFC)
- M. DiSanti (GSFC)
- D. Jaffe (U. of Texas)
- L. Keller (Ithaca College)
- V. Krasnopolsky (Catholic U. of America)
- K. Magee-Sauer (Rowan Univ.)
- S. Miller (Univ. College London)
- M. Mumma (GSFC)
- J. Najita (NOAO)
- R. Novak (Iona College)
- L. Prato (Lowell Obs.)
- M. Simon (SUNY Stony Brook)
- T. Stallard (Univ. College London).

2.1. Composition of Comets

Comets are the least altered objects from the birth of the Solar System providing the most direct means for determining the chemistry and conditions present during this formative period. Thus, the study of comets is intimately connected to fundamental research in astronomy including the formation, evolution and chemical inventory of our Solar System, physical conditions and composition of circumstellar disks (see §2.10), and the chemistry of the interstellar medium.

Infrared spectroscopy provides important information that is difficult or impossible to obtain from other methods, such as radio observations. This includes the direct detection of water (Dello Russo *et al.* 2004) and non-polar molecules such as CH_4, C_2H_2, and C_2H_6 (Mumma *et al.* 2001, Brooke *et al.* 2003, Weaver *et al.* 1999, Dello Russo *et al.* 2002, Magee-Sauer *et al.* 2002, Gibb *et al.* 2003, Kawakita *et al.* 2003). Several chemical groups have been potentially identified among the comets studied to date (Mumma *et al.* 2001, 2003; 2006; Villanueva *et al.* 2006). Observations to date suggest the presence of two distinct chemical groups in both principal dynamical reservoirs (Kuiper Belt, Oort Cloud), consistent with emerging views of dynamics in the protoplanetary disk (Tsiganis *et al.* 2005). However, other studies suggest a general diversity in comet composition that defies easy classification (Biver *et al.* 2002).

Obtaining a significant sampling of comets at infrared wavelengths has been hampered because CSHELL is outdated, and only very limited time is available to the broad community on NIRSPEC at Keck, and just a fraction of that for solar systems studies. Owing to the large fraction of time reserved for solar system studies at IRTF, iSHELL can characterize upwards of 100 comets during its operating lifetime, and can improve detection limits by at least a factor of ten due to its multiplex advantage. The combination will establish statistically significant population ratios for chemical groups in each dynamical reservoir. In addition to comet chemistry, isotopic ratios and nuclear spin temperatures in volatiles provide important clues for cometary formation histories. The measured D/H ratios and nuclear spin temperatures will constrain predicted radial gradients in organic chemistry, when coupled with models of disk chemistry. Comparison with dynamical models can then predict delivery of organics and water to young planets, for comparison with current inventories on Earth and Mars (e.g., D/H). The extension to disks around young stars can test the degree to which interstellar vs. nebular processing control the evolution of cometary organics and water.

Technical Discussion

iSHELL provides about a factor of two improvement in spectral resolution compared to CSHELL and NIRSPEC, greatly alleviating spectral confusion, and disentangling intrinsic features from telluric features. There are two main regions where studies will greatly benefit from higher spectral resolving power - near 3.0 μm (Figure 1 *A*), and between about 3.3–3.6 μm (Figure 1*B*, *C*). These confused spectral regions contain vibrational bands of many other species that could be detected with higher spectral resolving power and sensitivity provided by iSHELL (Dello Russo *et al.* 2006). Higher spectral resolution will increase line-to-continuum contrast and thus help with interpretation of known species in confused regions and also increase the potential number of detectable unblended lines for important less abundant species such as HC_3N, CH_3CCH, C_4H_2, HCOOH, CH_3CN, C_3H_8, C_2H_5OH.

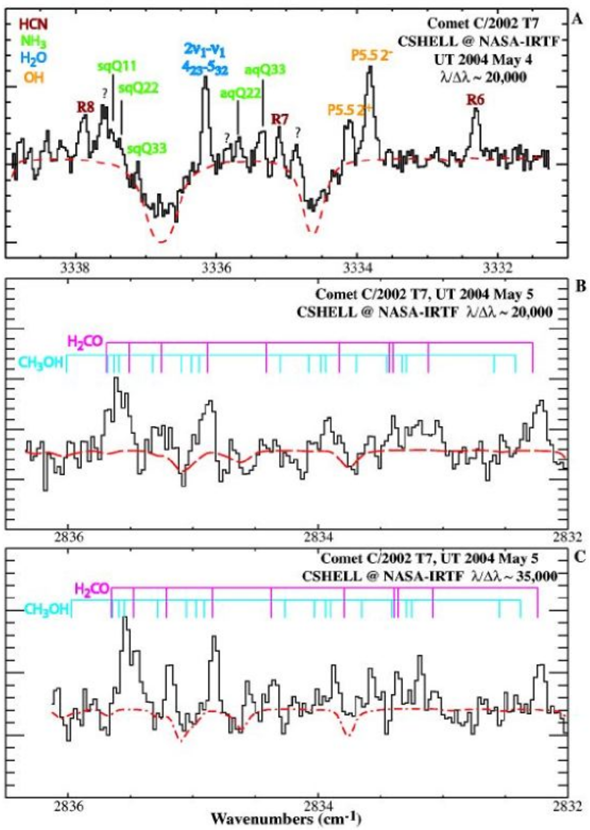

Figure 1. Infrared spectra of comet C/2002 T7 (solid traces) obtained with CSHELL in daylight. These figures illustrate the need for higher spectral resolving power. A synthetic model of atmospheric transmittance shown as dashed red traces. (***A***) Spectrum near 3.0 μm showing a high-density of lines due to different species (*R*~20,000). Spectra near 3.53 μm with (***B***) *R*~20,000, and (***C***) *R*~35,000 with CH_3OH and H_2CO expected line positions are noted. Spectral confusion in all regions will be greatly reduced with iSHELL (*R*~70,000) by providing higher line-to-continuum contrast and better separation of lines. The 15″ slit will allow distinguishing molecules that originate directly from the nucleus (e.g., C_2H_2, NH_3, CH_3OH, H_2CO) and from those that are produced or released as distributed sources in the coma (e.g., CO, H_2CO).

Table 2.1 Comet science drivers

Parameter	**Requirement**	
	Essential	**Optimum**
Resolving power (R)?	R=70,000	R=100,000
Wavelength coverage?	L-band, ~λ/20	
Target brightness, number of targets?	L= 8 mag arcsec^{-2}, ~100	L= 9 mag arcsec^{-2}, >100
Required S/N	100	
Spatial resolution?	0.5″ (360km at 1AU)	
Slit length?	15″	30″
Rotate slit?	Yes	
Sky subtraction?	Nod out of slit	
Standard star?	No. Use atmospheric model to remove telluric features	
Wavelength calibration?	Arcs or telluric features	
Acquisition?	IR imaging, daytime	
Guiding?	No. Non-sidereal tracking	Yes
Imaging?	LL′, to locate slit, photometry	

2.2. Detection of minor constituents in the atmosphere of Mars

The exploration of Mars is a major goal for the next decade within NASA's Science Mission Directorate. Spacecraft do not employ high-resolution spectrographs due to space and weight limitations. Thus ground-based observations using high-resolution spectroscopy provide unique and important data as well as a long baseline of observations not generally obtainable from space missions.

iSHELL offers significant advantages that may potentially revolutionize ground-based studies of Mars. An outstanding example of this is the recent detection of CH_4 (Mumma *et al.* 2007; see Figure 2). At present, only a single line of CH_4 can be sampled per setting. iSHELL would allow the entire CH_4 n_3 band to be sampled simultaneously. Higher resolving power would help to better separate the Martian lines from their terrestrial counterparts since a Doppler shift is needed to resolve the Martian spectral lines from their corresponding terrestrial lines.

Simultaneous mapping of HDO (near 3.7 μm) and H_2O (near 3.3 μm, Figure 2) will provide a precise value of D/H in water. Recent determinations of this ratio used HDO measurements from CSHELL and H_2O measurements from either spacecraft or CSHELL. This method has built-in limitations. With the slit placed along the rotation axis, latitudinal maps will be constructed; since both forms of water have different volatilities, questions relating to both annual and long term (geologic time) stability will be addressed.

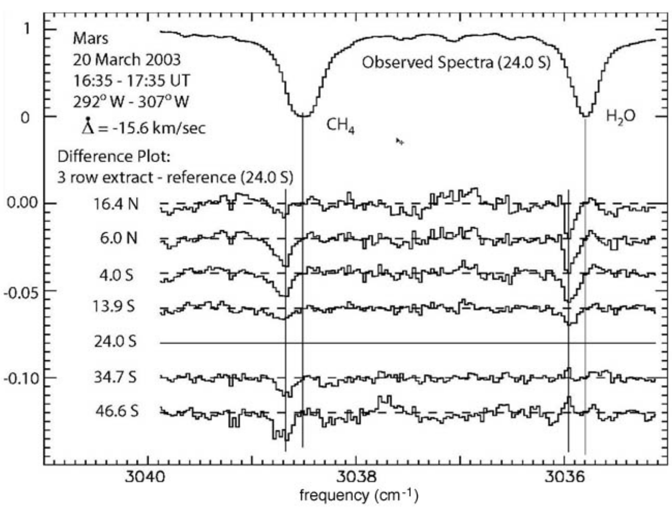

Figure 2. Methane and water absorption on Mars. The spectra were taken with CSHELL using a 0.5″ slit (R~ 35,000) centered at 3037 cm^{-1} (3.29 μm). The Doppler-shifted CH_4 and H_2O lines in the Martian atmosphere are indicated by the vertical lines to the left of the strong telluric line. The observed methane absorptions are less than 2% corresponding to a level ~10 ppb. Confirming observations are in progress.

Technical Discussion

iSHELL provides about a factor of two improvement in spectral resolution compared to CSHELL and NIRSPEC, greatly alleviating spectral confusion, and disentangling intrinsic features from telluric features. The slit should be long enough to cover the central meridian and ideally to allow nodding of the disk within the slit for sky subtraction. Efforts should be made to minimize scattered light, which fills in spectral features in varying degrees with CSHELL, NIRSPEC, and CRIRES.

Table 2.2 Mars atmosphere science drivers

Parameter	Requirement	
	Essential	Optimum
Resolving power?	R=70,000	R=100,000
Wavelength coverage?	L-band, ~λ/10	L-band ~λ/5
Target brightness, number of targets?	L≈2 mag arcsec^{-2}, Mars at opposition	
Required S/N	100	
Cadence	Minutes (planetary rotation in slit)	
Spatial resolution?	0.5″ (360km at 1AU)	
Slit length?	15″	30″
Rotate slit?	Yes	
Sky subtraction?	Nod out of slit	Nod in slit
Standard star?	No. Use atmos model to remove telluric features	
Wavelength calibration?	Arcs or telluric features	
Acquisition?	IR imaging	
Guiding?	Yes. Guidebox on disk	
Imaging?	nbL, to locate slit, photometry	

2.3. Ion winds and deposition in Jupiter's upper atmosphere: coordinated Juno-IRTF observations

The upper atmospheres of planets form a key interface between the planet itself and its space environment. In the case of magnetized planets, this space environment forms a magnetosphere, a region of space (partially) shielded from the solar wind, under the control of the planet's magnetic field. Earth and all the giant planets have magnetospheres: the Jovian magnetosphere is the largest structure in the Solar System with the exception of the solar wind. The upper atmosphere consists of a coexisting neutral thermosphere an ionized ionosphere, both of which play important roles in the magnetosphere-atmosphere interaction.

The Juno mission to Jupiter will place a spacecraft into a polar orbit that will allow both the magnetosphere and the most energetic and important regions of the planet's upper atmosphere – auroral/polar regions – to be studied in depth and at length for the first time. Juno arrives in July 2016 for a nominal mission duration of one year. This proposal is to use iSHELL to trace energy inputs from the magnetosphere into the upper atmosphere and to measure the ion winds generated. Our observing team of (Miller *et al.*) has been using emission from the key Jovian ionospheric component H_3^+ since this ion was first discovered in Jupiter's auroral/polar regions 25 years ago (Rego *et al.* 1999). Energetic electrons precipitating from the magnetosphere into the upper atmosphere form H3+: the ion is formed by the reactions:

$$H_2 + e^- \rightarrow H_2^+ + 2e^-$$
$$H_2^+ + H_2 \rightarrow H_3^+ + H$$

Thus the ion is a tracer of magnetospheric energy inputs into the atmosphere.

We have developed techniques that make use of the Doppler shifting of well-characterized emission lines in the *L′* window to map ion winds. Ion winds are signatures of electric fields and energy deposited by the magnetosphere. Our research has also shown that these ion winds generate considerable heating as a result of Joule heating and ion drag, generating neutral winds that – in turn – significantly modify the magnetosphere/atmosphere interaction. The energy generated in this way is of the order of 10^{14} Watts, several times the amount deposited by particle precipitation, and at least 100 times more that the global insolation absorbed in the upper atmosphere.

One of the key issues is to "calibrate" the various components of this interaction. This requires simultaneous measurements of plasma and magnetic field conditions in the Jovian magnetosphere, whilst monitoring the atmospheric response. Juno does have a EUV imager, which is sensitive to neutral H_2 emission from the lower thermosphere and upper mesosphere. However, it does not have the capacity to measure ion winds and the H_3^+ emissions from the middle thermosphere, where ionization is at its maximum, and magnetosphere-atmosphere coupling is most efficient and affecting.

We propose to use iSHELL in modes that will enable us to pick up key H_3^+ emission lines from which we can determine ion densities, temperatures, total emission (cooling) and wind speeds. These parameters used in conjunction with the 3-D, fully coupled, Jovian ionosphere-thermosphere-magnetosphere model that we run at University College London, will enable us to develop a complete picture of energy transfer and related dynamics in this complex and ever-changing system. iSHELL will provide enormous advantages over current observations through lowering of the Doppler shift limit to about 50 m s^{-1}, simultaneous imaging of the slit position on the object, greater spectral coverage, and increased signal-to-noise.

Technical case

The key H_3^+ emission lines we will use are Q-branch ro-vibrational transitions in the infrared-active, asymmetric stretch/bend n_2 manifold, corresponding to the molecule relaxing from v_2=1 to v_2=0. The strongest of these occur between 3.953 and 4.014 μm. These lines are very bright, and we will get S/N >10 in 60s exposure on the planet, if the iSHELL sensitivity is as good as the current CSHELL spectrograph. In addition to the fundamental n_2 lines, we will also observe several transitions from the $2n_2$ (l_2 =0,2) → n_2 hot band (which correspond to v_2 = 2→1), which also occur in the L7 and L8 grating setups. Other *L* windows that our settings will cover also contain H_3^+ fundamental and hot-band transitions.

We intend to set up iSHELL to obtain the maximum slit length, and to set the slit east-west across the planet (perpendicular to the noon meridian). We will raster scan the auroral/polar regions, starting with the slit slightly off the pole, and scanning in 1″ steps equatorward. At opposition, Jupiter will span about 48″ on the sky, and the full extent of the Jovian aurorae, which extend down to latitudes as low as 50° will be about 30″ east-west across the planet. Ideally we will use a 30″ long slit, as with the current CSHELL. We will also take a spectrum at the equator; although we cannot get the full limb-to-limb extent of the planet there, it gives us a good indication of the H_3^+ emission and ion properties on the body of the planet.

In order to get the most accurate measurements of the ion wind speeds (obtainable from the Doppler shifting of the H_3^+ lines), which also provide crucial information about the magnetospherically imposed electric fields in the upper atmosphere, we will use the highest spectral resolution. This will give us a major advance in accuracy over the current CSHELL measurements; this is vital for picking up the slower winds that occur in the Dark and Bright Polar Regions of the atmosphere, which connect to field lines that may be open to the solar wind, and through which JUNO will fly.

We will use a narrow-band *L* filter in the guide camera to obtain planetwide images of the thermal emission of Jupiter and, crucially, images of the H_3^+ emission in the auroral/polar regions. However, we will also need images taken through a narrow band filter (*R*~200) centered on 3.95 μm, to be taken immediately prior to and after our raster scans to assist with correcting the raw line shifts to subtract effects due to the uneven illumination across the slit. Offset guiding on a suitable star or Jovian moon will be required, as Jupiter is too large for the guider to centroid accurately.

Stellar spectra will be required for flux calibration. These usually take about 10 minutes elapse time, depending on the magnitude of available flux standards. Each narrow-band filter image will take about 60s to obtain. Each spectrum will take about 2 minutes, 60s on object and 60s on sky, and we expect the need about 10 spectra per hemisphere to get total coverage of the auroral/polar regions. Thus we expect to raster scan both hemispheres within an elapse time of 50-60 minutes, including time for properly positioning on the planet for each hemisphere. At opposition we will therefore be able to carry out 10 full scans per night, given a full night's observing.

Table 2.3 Jupiter's upper atmosphere science drivers

Parameter	**Requirement**	
	Essential	**Optimum**
Resolving power?	R=70,000 (4 km s^{-1})	R=100,000 (3 km s^{-1})
Velocity precision	100 m s^{-1}	50 m s^{-1}
Wavelength coverage?	*L*-band, ~λ/20	*L′*-band, ~λ/5
Target brightness, number of targets?	Bright	
Required S/N?	30	50
Cadence	Minutes (planetary rotation in slit)	
Spatial resolution?	0.5″ (2000 km at 5AU)	
Slit length?	15″	60″
Rotate slit?	Yes	
Sky subtraction?	Nod out of slit	
Standard star?	Hot star	
Wavelength calibration?	Arcs or telluric features	
Acquisition?	IR imaging	
Guiding?	No. Non-sidereal tracking	
Imaging?	*L′*, nbL (0.5%)	

2.4. The atmospheres of Jupiter and Saturn

The 5-μm window provides a wealth of information about the gas composition and cloud structure of the troposphere of Jupiter. Chemical models of Jupiter's cloud structure predict three distinct layers: an NH_3 ice cloud near 0.5 bars, an NH_4SH cloud formed from a reaction of NH_3 and H_2S at 2 bars, and a massive water ice cloud near 4 to 6 bars (Weidenschilling *et al.* 1973). Jupiter exhibits remarkable spatial structure at 5 μm due to the variable opacity of these three cloud layers. Thermal emission at 5 μm originates near the 6- to 8-bar level where τ=1 due to pressure-induced H_2. In a relatively cloud-free Hot Spot, such as where the Galileo Probe entered in 1995, the radiance is an order of magnitude higher than in adjacent cloudy regions. As shown in Figure 3, images at 5 μm reveal information on the morphology of Jupiter's cloud features (de Pater *et al.* 2010, 2011), but in order to obtain the pressure level of the clouds, it is necessary to obtain spectra at high spectral and spatial resolution.

Figure 3. Mosaiced 5μm view Jupiter's northern hemisphere taken with NIRC2/Keck. The north polar cap contains bright rings surrounding small ovals seen in reflected sunlight.

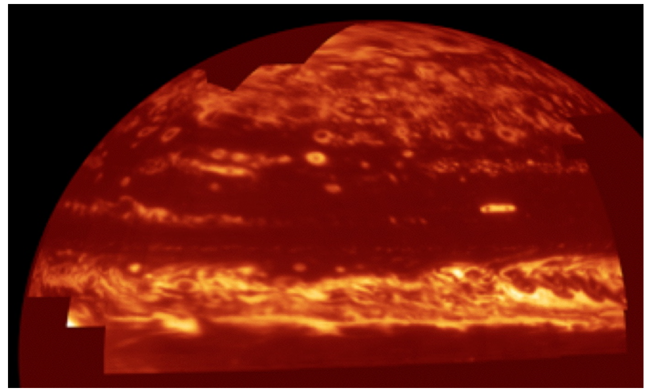

Water clouds on Jupiter are very difficult to study. Water ice has been detected in isolated regions where active convection lofted the ice well above its condensation level (Simon-Miller *et al.* 2000), but water clouds are generally hidden by overlying NH_3 and NH_4SH clouds. However, spectroscopy at 5 μm can probe levels below Jupiter's NH_4SH clouds, unless these clouds are completely opaque. Spectrally resolved line shapes at high spatial resolution allow us to identify the altitude of water clouds on Jupiter even when overlying NH_3 clouds and NH_4SH clouds are also present. Absorption lines at 5 μm are pressure-broadened due to collisions with 2 to 6 bars of H_2 therefore, they are fully resolved at R ~ 20,000. However, discrimination against telluric features is much improved at iSHELL resolving powers. Our measurements of the pressure of the water clouds will provide lower limits to the deep abundance of water vapor in Jupiter's atmosphere (Wong *et al.* 2008), a quantity that is of great cosmochemical importance as a constraint on planetary origins.

Existing CSHELL data provide tantalizing evidence for clouds at the pressure level where water condenses on Jupiter. With its much great wavelength coverage iSHELL could confirm their presence in Jupiter's zones and in other regions on Jupiter, such as the Great Red Spot and Oval BA. Beyond demonstrating the existence of water clouds, measurements of their pressure levels will constrain the mixing and vertical transport in the water condensation region on Jupiter. We also will measure the spectral line shape of CH_3D in hot spots, zones, and inside and outside of discrete cloud features to establish the presence and pressure levels of water clouds on Jupiter. Deuterated methane is an excellent tracer of cloud structure because methane does not condense on Jupiter, unlike NH_3. Variations in the strength and shape of CH_3D lines between belts and zones on Jupiter are only due to changes in cloud structure, not gas concentration. Our observations of water clouds will be complementary to data to be acquired by the Juno mission en route to Jupiter, which will measure O/H via microwave radiometry as well as column abundances of H_2O using the Juno IR Auroral mapper (JIRAM, Adriano *et al.* 2008). These ground-based data will add great value to the interpretation of the JIRAM results by providing an atmospheric model derived from data at 100 times higher spectral resolution.

Saturn's five-micron "cold spots" have been seen in NSFCAM images by Yanamandra-Fisher *et al.* (2001), and more recently with Cassini/VIMS (Baines *et al.* 2005). As both of these data sets have shown, Saturn's appearance at 5 μm is mottled and lacks the more zonally symmetric appearance of the upper-most cloud deck seen in visible light images. The manifestation of hot and cold spots of Saturn is likely a result of discrete clouds of varying thickness that modulate the thermal emission escaping from Saturn's deep atmosphere.

The detection of spatial variations in Saturn's trace constituents would be significant as they would be indicative of localized dynamical processes. Saturn's atmospheric transmission windows between 2.5–5 µm are defined predominantly by CH_4 and PH_3 absorption bands. Of particular interest is PH_3 absorption, which modulates a significant fraction of Saturn's reflectivity between 4.5 and 5.4 µm (Larson *et al.* 1980). However, there are peaks in the Saturnian radiance near 5 µm, where PH3 does not absorb, that are defined solely by NH_3 absorption features (see Figure 4). Phosphine is a disequilibrium species, thus any spatial variation in PH_3 may be linked to variations in upwelling from the deep atmosphere. Unlike PH3, variations in NH_3 would be associated with spatial variations in cloud formation. The Cassini IR Spectrograph-derived PH_3 abundance at 1 bar provides a critical boundary condition for modeling the IRTF spectra at 5 µm, which probe deeper levels. CSHELL spectra show dramatic differences between Saturn's south pole and equator at 5 µm. We interpret this as evidence for thicker NH_4SH clouds at the equator. Analysis of these line shapes will constrain the optical thickness and pressure level of the cloud condensate. Preliminary models suggest that the cloud responsible for modulating the shape of these PH_3 and PH_3 lines resides around the 3-bar level and thus would be identified with NH_4SH rather than NH_3, which condenses at the 1-bar level. With higher resolving power and much greater spectral coverage iSHELL open many more spectral features to analysis and modeling.

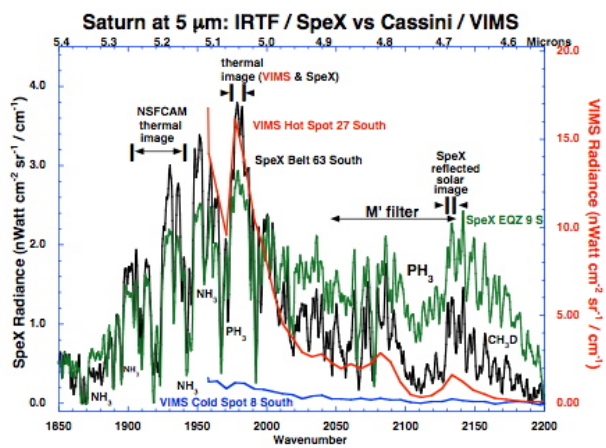

Figure 4. Spectra of Saturn's 5µm window from SpeX and Cassini/VIMS showing useful continuum windows for imaging the planet. iSHELL image cubes will be used to model the full 5µm spectrum. Since individual lines can be isolated much higher contrast can be achieved than with conventional imaging.

Technical case

Jupiter and Saturn will be spectrally mapped by scanning the longest slit across the disk in steps of the slit width. The big advantage of iSHELL is that only one grating position is required to measure multiple lines compared to CHSELL that can only do one line per setting. Simultaneous M′ imaging is done with the IR guider.

Table 2.4 The atmospheres of Jupiter and Saturn science drivers

Parameter	Requirement	
	Essential	**Optimum**
Resolving power?	R=50,000	R=100,000
Wavelength coverage?	M-band, ~λ/10. $\lambda \leq 5.3$ μm	M-band ~λ/5
Target brightness, number of targets?	Bright – itime ~minutes	
Required S/N	100	
Cadence	Minutes (planetary rotation in slit)	
Spatial resolution?	0.5″ (2000 km at 5AU)	
Slit length?	15″	30″
Rotate slit?	Yes	
Sky subtraction?	Nod out of slit	Nod in slit
Standard star?	No. Use atmospheric model to remove telluric features	
Wavelength calibration?	Arcs or telluric features	
Acquisition?	M′ imaging	
Guiding?	Off-axis star and slit scan	
Imaging?	M′ imaging to locate slit	

2.5. Probing the atmospheres of hot giant planets

The recent detection of thermal emission from several transiting exoplanets using Spitzer (Deming *et al.* 2005, 2006, Charbonneau *et al.* 2005) proves that the infrared flux from these exoplanets is significant (up to 0.005 of the stellar flux). Doppler deconvolution is a technique that can be used with iSHELL to detect the spectral signatures of these planets. The orbital radial velocity of a planet orbiting a solar-type star with a 4 day period approaches 150 *sini* m/sec, causing a large periodic wavelength displacement of the planetary lines (see Figure 5). Since the planetary molecular lines are numerous, narrow, and spread over large regions in wavelength, their detection by Doppler deconvolution requires a high resolution IR spectrograph with large wavelength coverage.

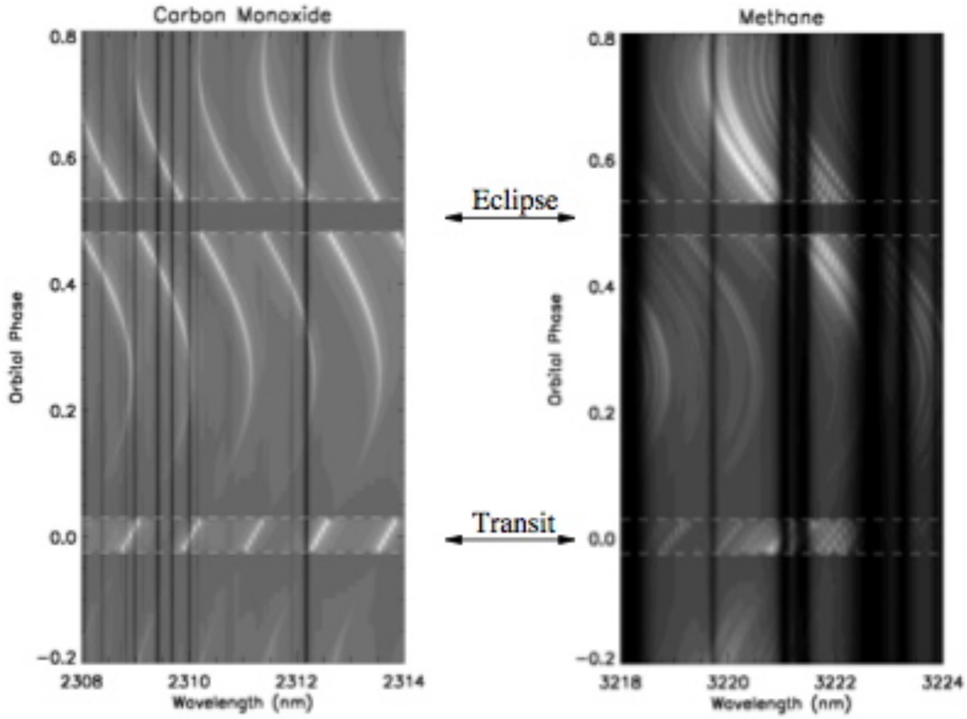

Figure 5. CO and methane models at K and L plotted as a function of wavelength and orbital phase. The vertical stripes are contaminating telluric features (Snellen *et al.* 2010).

Technical case

A successful detection of CO in the atmosphere of exoplanet HD209458b is reported by Snellen *et al.* (2010) using CRIRES on VLT. The observations covered 180 min. transit plus a 40 and 90 min. baseline before and after the event. Fifty-one spectra were obtained with wavelength coverage of 2.2291-2.349 μm (with some gaps due to the unfilled focal plane) at a resolving power of about 80,000. Methane and water telluric lines dominated the spectra and an important part of the reduction process involves the removal of this telluric contamination, which varies with airmass. CO was detected at 5.6σ. These are difficult observations

Although IRTF is a small telescope iSHELL is still competitive due to its increased wavelength coverage with signal to noise ratio given by:

$$S/N \infty\ D \times (\#lines)^{1/2}$$

For signal-limited observations and where D is the diameter of the telescope. Compared to CRIRES, iSHELL can cover about 3-6 times more wavelength range and therefore that many more lines. It is important to discover more bright transits.

Table 2.5 Atmospheres of hot giant planet science drivers

Parameter	Requirement	
	Essential	**Optimum**
Resolving power?	R=50,000 (6 km s^{-1})	R=100,000 (3 km s^{-1})
RV stability and relevant timescale?	50 m s^{-1}, over hours	5 m s^{-1}, over hours
Wavelength coverage?	*K* and *L*, ~λ/10	K and L, ~λ/5
Target brightness, number of targets?	*K*~5, *L*~4. Candidate stars ~10	
Required S/N?	~200 per 120 s	
Cadence	Minutes for several hours?	
Spatial resolution?	Point source	
Slit length?	15″	
Rotate slit?	No	
Sky subtraction?	Fit sky along slit	
Standard star?	No	
Wavelength calibration?	Arcs or telluric features	
Acquisition?	NIR imaging	
Guiding?	Off-axis guiding	On-instrument guiding but not on spill-over from slit
Imaging?	*JHKL* photometry	

2.6. Finding the youngest planets with iSHELL

The discovery and characterization of exoplanets has marked the past two decades as an exciting new era of insight into the formation of solar system analogues. Recent surveys have reported planets around high-mass stars, low-mass stars, younger stars, and in complex multiple systems (e.g., Johnson *et al.* 2008; Butler *et al.* 2006; Setiawan *et al.* 2007; Marois *et al.* 2008). In spite of this tremendous progress, however, little is known about the youngest generation of planets. This is key because the age at which planets form will dictate the details of the formation mechanism: the core accretion model requires several Myr to produce Jupiter mass planets whereas gravitational instabilities can yield planets on timescales of <~1Myr (e.g., Papaloizou *et al.* 2007; Durisen *et al.* 2007).

We propose to carry out a radial velocity search for the youngest planets with iSHELL on the IRTF. This requires observations of young (about a few Myr) stars in nearby star forming regions. Such young targets manifest copious stellar activity and typically appear to be highly spotted. The action of a large spot on an inclined, rotating young star mimics the radial velocity modulation expected from the reflex motion induced by a planet (Huerta *et al.* 2008). By observing the same targets in visible and infrared light, we can distinguish between spots and planetary mass companions on the basis of the radial velocity variability amplitude. Cool spots show a much higher contrast with the warmer stellar photosphere in visible light than in the infrared, where the spectral energy distributions of both spot and photosphere are in the Raleigh-Jeans regime. Thus, the apparent radial velocity modulation of a spotted star has a significantly higher amplitude in visible vs. infrared light. In contrast, the radial velocity modulation amplitude induced by a planet is constant in the visible and infrared.

Using visible light observations at the McDonald and Kitt Peak observatories we are surveying ~100 young stars in the Taurus star forming region for radial velocity variability. Our IRTF+CSHELL observations to date of candidates displaying periodic radial velocity modulation have yielded much reduced amplitudes in the infrared, indicative of star spots (Prato *et al.* 2008). Because the spectral range of CSHELL is extremely limited (~700 km/s, $\lambda/400$), relatively few spectral lines are simultaneously observable. Combined with the relative inefficiency of this instrument, our precision on our young star radial velocity measurements is at best 200 m/s. With increased efficiency and a factor of 30 improvement in spectral range, iSHELL will provide an increased precision of about a factor of 5 (assuming a uniform distribution of spectral lines across the observed wavelength range and an increase in precision proportional to the square root of the number of lines observed) to ~40 m/s.

We are now beginning to use infrared observations to focus on targets with large radial velocity RMS at visible light wavelengths, but which do not necessarily show periodic behaviour. These targets are the most likely to manifest a combination of spots and planetary companion(s). To date we have observed about 4 of these non-periodic variables; dozens of targets remain, many of which will be ideally observed with iSHELL.

Technical case

Stellar radial velocities are measured with respect to simultaneously observed telluric absorption lines. We fit the observed spectrum with a model consisting of a stellar template spectrum (either the NSO sunspot atlas or a synthetic spectrum) multiplied by the NOAO telluric atlas. The stellar template and telluric atlas are shifted relative to each other and appropriately scaled until a best fit is achieved in a χ^2 sense (Blake *et al.* 2007, 2008; Prato *et al.* 2008). A resolving power of 70,000 (0.38" slit) would be ideal for these observations; 35,000 is adequate. The higher resolution enables finer sampling of spectral lines, and therefore more precise fitting of the observed line profiles. A slit length of at least 6" (preferably 10") to enable on-slit nodding is necessary for sky and bad pixel subtraction. Because of the small slit width required for R=70,000, auto-guiding stability of <0.1″ is necessary to avoid large slit losses.

Because radial velocity precision is paramount to this project, observations that minimize the changes to the instrument are highly preferable. Thus, we will not change any settings (slit, filter, etc.) between observations, particularly between observations of flat field and comparison lamps and the target objects. We will obtain comparison lamps at intervals throughout an observing night to measure the impact, if any, of flexure on the dispersion. In the ideal case, we will obtain darks, flats, and comparison lamps before sunset, focus after sunset, move to target objects, and acquire data. With a slit-viewing camera we will maintain the slit setting used for the flat lamps even during target acquisition and thus will not require repeated observations of flats during the night. For comparison, we will obtain another set of flats after sunrise. Because we will use the telluric absorption lines inherent in the observed spectra for wavelength, and hence radial velocity, zero-point measurements, density of comparison lamp lines is not a priority; one line per 0.004 μm is adequate.

Better radial velocity precision can be achieved with a gas cell of the type currently being used in CSHELL by Plavchan *et al.*

Table 2.6 Young planet science drivers

Parameter	Requirement	
	Essential	**Optimum**
Resolving power (R)?	R=35,000	R=70,000
Wavelength coverage?	*K*-band, ~λ/10	
Target brightness, number of targets?	1 hour at *K*=9.5, ~100 targets?	
Required S/N	100	
RV precision	< 40 m/s (weeks)	< 10 m/s (weeks)
Spatial resolution?	Point source	
Slit length?	6″	15″
Rotate slit?	No	Yes
Sky subtraction?	Nod in slit	
Standard star?	Use telluric features as wavelength reference	
Wavelength calibration?	Arcs and telluric features ~20 m/s precision Gas cell ~5 m/s precision	
Acquisition?	IR imaging	
Guiding?	Yes, spill-over from target in slit	On-instrument or off-axis guiding
Imaging?	*JHK* photometry?	

2.7. Young star binaries and pre-main sequence model calibration

Because mass is the key determinant of stellar evolution, its measurement is critical to tests of models (e.g., Hillenbrand & White 2004). Observations of young spectroscopic binaries provide measurements of dynamical mass ratios (e.g., Prato *et al.* 2002) and, in concert with high angular resolution observations, individual young star masses (Schaefer *et al.* 2008). Systems in which the stellar masses differ significantly are particularly important to test a large area of model parameter space. High resolution, near-infrared spectroscopy with iSHELL will provide a powerful tool for detecting low mass secondaries in spectroscopic binaries. Mass scales as a steeper function of luminosity in visible light compared to the infrared, thus the secondary to primary flux ratio is greater at longer wavelengths, favoring the detection of cool secondaries. This technique enables the calibration of pre-main sequence evolutionary models and provides input for theories of binary star, brown dwarf, and exoplanet formation mechanisms.

Technical case

The technique requires cross correlating a range of template spectra of stars of different spectral types with the observed spectra to find the best fit to the primary and secondary velocities. For this purpose a library of template spectra will be obtained with iSHELL. The sensitivity of the technique improves with the number of features observed ($\#lines^{1/2}$) and therefore with the spectral range. However, telluric contamination can limit the spectral range so it is important to mitigate the effects of telluric contamination. Working at higher resolving powers will provide better discrimination of telluric features and the use of a standard star or telluric model should help significantly with their removal.

Table 2.7 Young binaries science drivers

Parameter	Requirement	
	Essential	Optimum
Resolving power?	R=50,000 (6 km s^{-1})	R=70,000 (4 km s^{-1})
RV stability and relevant timescale?	200 m s^{-1}, over a few nights	50 m s^{-1}, over a few nights
Wavelength coverage?	*J*-, *H*- and *K*-band, ~λ/10	
Target brightness, number of targets?	1 hour *J*, *H* and *K* ~10 ~ 100 binary systems?	
Required S/N?	100	
Cadence	A few epochs per night for a few nights?	
Spatial resolution?	Point source	
Slit length?	15″	
Rotate slit?	Yes (binaries)	
Sky subtraction?	Fit sky in slit	
Standard star?	Yes or fit telluric features using a model atmosphere	
Wavelength calibration?	Arcs or telluric features	
Acquisition?	IR imaging	
Guiding?	Yes, spill-over from target in slit	
Imaging?	*JHK* photometry?	

2.8. Structure and kinematics of protostellar envelopes

Individual stars are believed to form in optically opaque (A_V > 1,000 mag.) rotating molecular cores of dimension ~0.1 pc. To date, these protostellar cores have been studied primarily at mm and sub-mm wavelengths, and largely in nearby (d < 500 pc) star-forming regions at spatial resolutions typically corresponding to 1,000s of AU. Such observations provide a measure of the core mass and large-scale morphology, and kinematic information sufficient to diagnose the onset of gravitational collapse.

At the earliest evolutionary phases, these cores are sufficiently opaque as to preclude detection of the forming star and its associated circumstellar accretion disk even at mid-infrared wavelengths. The presence of the star-disk system can be inferred from (a) measurement of dust-reprocessed mid- and far-IR emission from which the total luminosity of the forming star and its accretion disk can be inferred; and (b) the kinematic signatures of collimated molecular outflows thought to arise from a magnetically-driven wind originating at or near the boundary between the stellar magnetosphere and a circumstellar accretion disk. At later stages in stellar assembly, the optical depth of the envelope decreases, and emission from the star-disk-outflow system can be observed, first at mid-IR wavelengths, and later at shorter wavelengths.

A fundamental issue that must be addressed is the linkage between the mass of a forming star and the initial conditions in the natal proto-stellar core giving birth to a star-disk system. Specifically, what is the relationship between the core mass accretion rate (presumably determined by the thermal plus turbulent speed in the core) and the mass of the emerging star? To answer this question requires measuring mass accretion rates for cores surrounding YSOs spanning a range of masses/luminosities.

At *R*=70,000 iSHELL will enable spectroscopic analysis of star-forming cores for a significant number of cores in nearby star-forming regions. High-resolution spectra using CO fundamental absorption as a diagnostic can be used to map temperature, density and velocity along the line of sight through the protostellar core to the spatially unresolved inner parts (r < 1 AU) of the star-disk system (which serves as the bright 'background' against which these features can be measured). An illustration of the potential of such measurements is provided by the pioneering study of Scoville *et al.* (1983) for the Becklin-Neugebauer source – a massive ($M > 10\ M_{\odot}$) proto-star located in the Orion star-forming complex. These authors used R~50,000 spectra to obtain profiles for a large number of absorption lines arising in the CO fundamental band – see Figure 6. In turn, these profiles mapped both the velocity field and density distribution along the line of sight to BN – leading to the only extent determination of mass inflow rate from a proto-stellar core to a star-disk system: a critical quantity for assessing the relationship between resulting stellar mass and proto-stellar conditions.

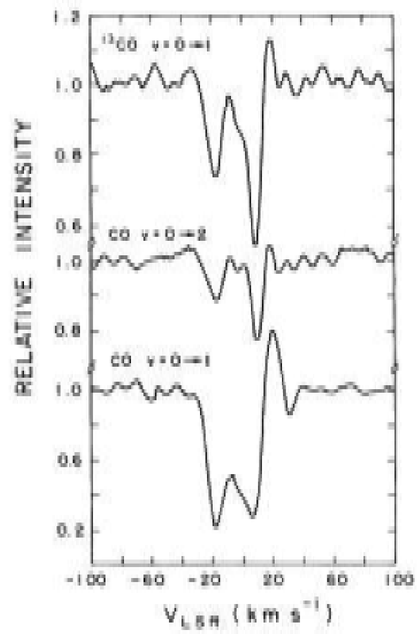

Figure 6. Profiles of CO fundamental band absorption features obtained by Scoville et al. (1983) from high-resolution (R~50,000) observations of the Becklin-Neugebauer Object – a high-mass proto-star deeply embedded within an optically opaque core. Observations of several tens of these profiles enabled Scoville et al. to derive temperature, density and velocity structure in the proto-stellar core and to derive the first quantitative estimate of mass inflow rate from a proto-stellar core to a forming star-disk system.

Technical case

Figure 7 provides an indication of the range of sources accessible to iSHELL on IRTF. The green-shaded histogram depicts the distribution of observed fluxes among sources in the Ophiuchus molecular cloud complex that are still surrounded by optically-opaque ($A_V > 50$ mag) proto-stellar envelopes (so-called 'Class I sources') - the focus of this proposed study. The estimated bolometric luminosities of these sources ranges from 0.1 to 30 $L_{\odot}$; associated forming stars are likely to have masses in the range 0.1 to 2 $M_{\odot}$. The superposed red line indicates the limiting flux for a 3-hr integration, yielding S/N=50 in the continuum at a resolution R=70,000. About half of the Class I sources in Ophiuchus are observable.

Figure 7. Histogram depicting (a) frequency distribution of source brightness for YSOs surrounded by accretion disks (dark grey) in the Ophiuchus molecular complex (b) distribution of source brightness for star-disk systems surrounded by optically-opaque in-falling envelopes (green; Class I sources). The red line represents the approximate sensitivity limit of iSHELL (M′=6.3, 3 hr, S/N=50) at the 4.6-µm CO fundamental band for spectra adequate to diagnose the temperature, density and velocity structure of in-falling envelopes and to derive mass accretion rates. About 30% of all the YSOs in Ophiuchus are accessible.

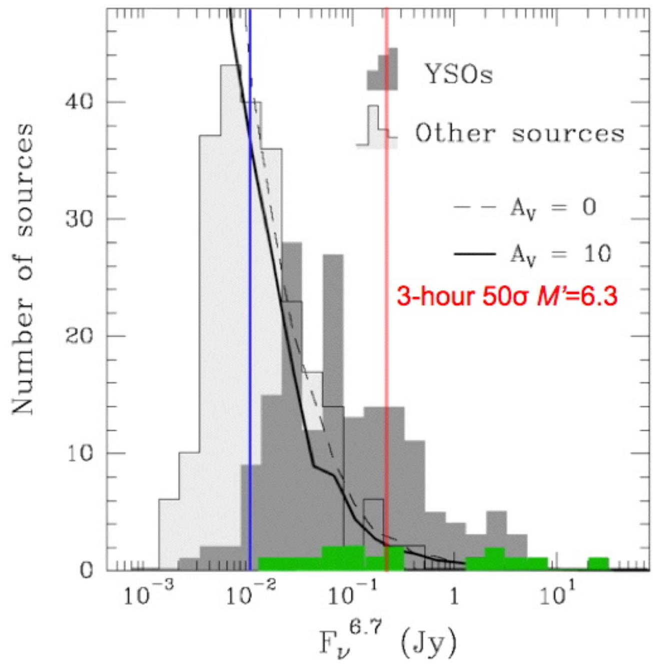

Table 2.8. Protostellar envelopes science drivers

Parameter	Requirement	
	Essential	Optimum
Resolving power?	R=35,000 (8 km s^{-1})	R=70,000 (4 km s^{-1})
Wavelength coverage?	M′-band, ~λ/10	
Target brightness, number of targets?	3-hour *M′*=6.3, ~10 Class I in Ophiuchus,	
Required S/N?	30	100
Spatial resolution?′	Point source	
Slit length?	15″	
Rotate slit?	No	
Sky subtraction?	Nod in slit	
Standard star?	Yes	
Wavelength calibration?	Arcs or telluric features	
Acquisition?	*KL′M′* imaging	
Guiding?	*K*-band on source or offset	
Imaging?	*KL′M′* photometry	

2.9. Protostellar evolution

Very young (< a few Myr old) protostars represent the earliest observable stages of star and planet formation and are thus key targets for understanding these processes (Greene & Lada 2000). Unfortunately, cool surface temperatures, high obscuration, and copious non-photospheric emission make it difficult to study these objects at optical wavelengths (e.g., White & Hillenbrand 2004). The high resolving power of iSHELL in the infrared provides good sensitivity to absorption lines necessary for the determination of effective temperature, rotational line broadening, and continuum veiling. From such measurements we can estimate protostellar masses, rotation rates, and properties of the circumstellar environments, compare these values with those predicted from models, and clarify how the youngest stars evolve (Doppmann *et al.* 2005; White *et al.* 2007).

Table 2.9 Protostellar evolution science drivers

Parameter	Requirement	
	Essential	**Optimum**
Resolving power?	R=50,000 (6 km s^{-1})	R=70,000 (4 km s^{-1})
Wavelength coverage?	K λ/10, L λ/20	
Target brightness, number of targets?	1 hour at K ~9.6, ~ 100 stars? 1 hour at L ~7.7, ~ 100 stars?	
Required S/N?	100	
Spatial resolution?	Point source	
Slit length?	15″	
Rotate slit?	Yes (binaries)	
Sky subtraction?	Nod in slit	
Standard star?	Yes	
Wavelength calibration?	Arcs or telluric features	
Acquisition?	IR imaging	
Guiding?	Yes, spill-over from target in slit	
Imaging?	JHKLM′ photometry?	

2.10. Magnetic fields and rotation – a key to understanding the accretion process

The powerful magnetic fields in YSOs play a role in the accretion process, in the evolution of protoplanetary disks, and in the transfer of angular momentum. Observations of Zeeman sensitive lines in the near-IR over the past several years with CSHELL have shown that classical T Tauri stars have organized magnetic fields of several kilogauss (Johns-Krull & Valenti 1996). It is probable that these powerful magnetic fields couple the star to its disk during the early part of the pre-main sequence period and have a significant influence on stellar rotation. In the earliest phases, the magnetic field couples the stellar rotation to the Keplerian rate at the inner edge of the disk. As accretion and angular momentum transport move this inner edge outward, the stellar rotation slows. As the disk dissipates however, the field no longer couples it to the star and accretion causes rotation rates to increase again (Shu *et al.* 1994). High resolution spectral observations over a broad wavelength range, coupled with disk models made from Spitzer SEDs will test this fast-slow-fast picture. The broad coverage and high resolving power of ISHELL will allow observations of many Zeeman-sensitive lines to determine magnetic fields and, at the same time, many lines with small Lande g factors that will allow observers to measure *vsini* for the same stars.

Technical case

Thousands of magnetically sensitive and insensitive photospheric lines are available for stellar magnetometry, both from atomsand molecules. Around 2.22 µm for instance, 3 Ti I lines @ 2.221, 2.223 & 2.227 µm (w/ respective Landé factors of 2.08, 1.66 and 1.58), One Sc I line at 2.226 µm (w/ Landé factor of 0.50), as well as the magnetically insensitive CO overtone lines around 2.3 µm (to calibrate Doppler broadening) are regularly used to estimate magnetic field strengths in protostars (e.g. Johns-Krull 2007, ApJ 664, 975; Johns-Krull *et al.* 2009, ApJ 700, 1440). Obviously, lines in the *K* band are most interesting given the increased Zeeman splitting resulting from the longer wavelength. Concerning accretion proxies, Brγ (2.17 μm) is a reliable tracer of accretion, showing minimal contamination by outflows as opposed to Hα. Getting all these lines with one setting avoids problems with variability, which is optimum for veiling corrections.

Assuming a typical *K* magnitude of about 10 (typical for Class I protostars) and a total exposure time of about 1 hr per star and per visit (yielding S/N~100), monitoring about 10 stars and 20 rotation phases (to be able to disentangle rotational modulation from intrinsic variability - usually very significant in protostars) requires a total observing time of about 5 nights per year for 5 years.

Table 2.10 Magnetic fields science drivers

Parameter	Requirement	
	Essential	Optimum
Resolving power?	R=50,000 (6 km s^{-1})	R=70,000 (4 km s^{-1})
Wavelength coverage?	*H* and *K* λ/10	λ/5
Target brightness, number of targets?	1 hour J, H and K ~10 ~ 10s of stars?	
Required S/N?	100	
Spatial resolution?	Point source	
Slit length?	15″	
Rotate slit?	No	
Sky subtraction?	Nod in slit	
Standard star?	Yes	
Wavelength calibration?	Arcs or telluric features	
Acquisition?	IR imaging	
Guiding?	Yes, spill-over from target in slit	
Imaging?	JHK photometry?	

2.11. Preplanetary disks and astrobiology

One of the key approaches to reconstruct the formation and early evolution of the Solar System, and to understand the origin of diverse exoplanetary systems, is to study the structure and chemistry of protoplanetary disks around young stars. Direct measurements of the gas in preplanetary disks are necessary to infer the conditions present in the presolar nebula, to distinguish among theories for planet formation, and to determine the likelihood of forming solar systems like our own. Measurements of the chemical abundances in protoplanetary disks, and comparisons to comets (§2.1) and molecular clouds, will help to determine the role of chemical processing and material transport, and lead to a better understanding of the origin of volatiles in the Solar System.

While continuum measurements probe the dust, and low-resolution spectroscopy can measure ice and solid-state features, the key tool for the study of the gas component is high-resolution infrared spectroscopy. In recent years, near-infrared molecular spectroscopy has developed as a major diagnostic of the chemical and thermal structure of inner disks. Work to date has focused on studies of the fundamental and overtone transitions of CO (Najita *et al.* 2003, Carr *et al.* 2001, Brittain *et al.* 2003, Blake & Boogert 2004) and near-infrared transitions of H_2O and OH (Carr, Tokunaga & Najita 2004). The pioneering work in this area was carried out at the IRTF with CSHELL.

An IRTF key project for preplanetary disks would consist of echelle spectroscopy in the 2-5 μm wavelength region of a large number of star-disk systems. This spectral region contains transitions of numerous molecules of great interest for characterizing the structure and chemistry of disks, including H_2O, OH, CH_4, C_2H_2, C_2H_6, HCN, and CH_3OH. Spectroscopy in the *K* band would yield a variety of related information, including the mass-accretion rate, the near-infrared veiling excess, and the stellar magnetic field. The excitation temperature and column density of individual molecules can be mapped as a function of radius by modeling the velocity-resolved line profiles, giving data on chemical abundances, ionization fractions, and turbulence. When these data are coupled with realistic models of the thermal, chemical and excitation structure of disk atmospheres, one can unravel the vertical disk structure and ascertain the dominant chemical and heating processes.

The origin and evolution of organic molecules and water are central to understanding the formative aspects of young planets, especially of environments suitable for the emergence and sustenance of life. A key question is: can preplanetary disks synthesize and retain complex molecules of biological significance, i.e., the "building blocks" of life? We can address this question observationally by studying the molecular content of young, planet-forming disks to provide insights into the disk chemistry. Measurements of organic molecules in disks, and comparisons to those in comets and molecular clouds, will fill in the missing link in our understanding of the chemical evolution of organic and prebiotic material and assess the disk's ability to synthesize precursor molecules. The *L* band contains transitions numerous hydrocarbons (e.g. CH_4, C_2H_2, C_2H_6, HCN, CH_3OH – see, for example Figure 8) and requires resolving powers of R~100,000 for optimum discrimination against the forest of telluric features at these wavelengths. iSHELL will provide both the high spectral resolving power needed to sample specific gases (and their rotational temperatures) and the broad spectral grasp needed to sample multiple species simultaneously (water, organics, nitriles, and deuterated isomers).

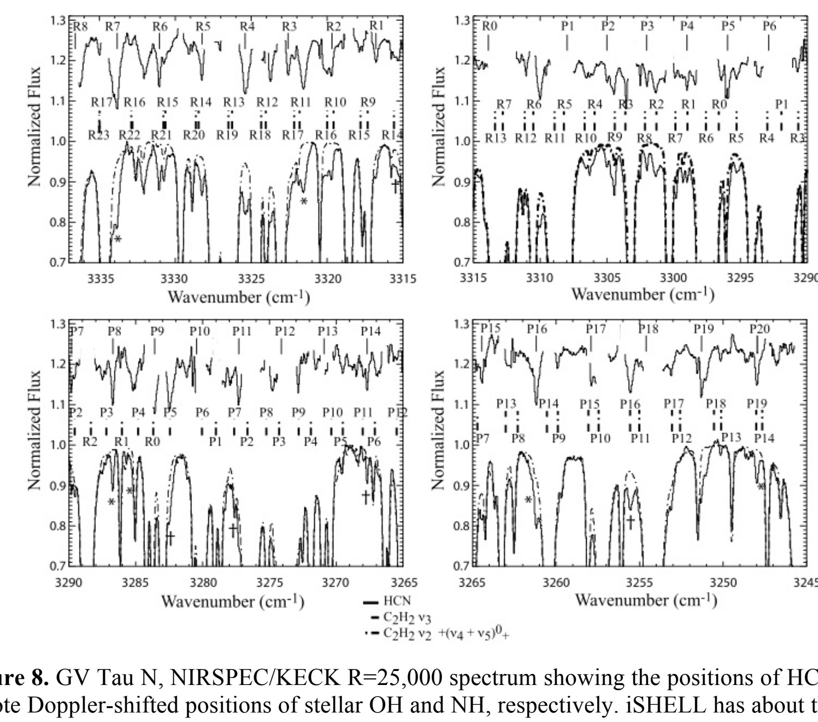

Figure 8. GV Tau N, NIRSPEC/KECK R=25,000 spectrum showing the positions of HCN and C_2H_2 lines. Asterisks and crosses denote Doppler-shifted positions of stellar OH and NH, respectively. iSHELL has about three times the resolving power and one-shot spectral coverage (Gibb *et al.* 2007).

Table 2.11 Preplanetary disk and astrobiology science drivers

Parameter	Requirement	
	Essential	**Optimum**
Resolving power?	R=50,000 (6 km s^{-1})	R=100,000 (3 km s^{-1})
Wavelength coverage?	K-band~λ/10, L-band ~λ/20, M-band ~λ/15	
Target brightness, number of targets?	1 hour at K ~9.6, ~ 100 stars? 1 hour at L ~7.7, ~ 100 stars? 1 hour at M' ~5.4, ~ 100 stars?	
Required S/N?	100	
Spatial resolution?	Point source	
Slit length?	15″	
Rotate slit?	Yes (binaries)	
Sky subtraction?	Nod in slit	
Standard star?	Yes. Or use atmospheric model to remove telluric features Measure continuum shape	
Wavelength calibration?	Arcs or telluric features	
Acquisition?	IR imaging	
Guiding?	Yes, spill-over from target in slit	
Imaging?	*KLM′* photometry (targets variable)	

2.12. A stellar library

The 1-5 μm spectral region is key for observing cool phenomena, including disks, planets, or the extended atmospheres of evolved stars. Electronic transitions of atoms, and in the case of molecules rotation-vibration transitions, produce lines in the near-infrared (NIR), among them indicators for obtaining isotopic ratios and resonance lines of s-process and rare earth elements. For the coolest stars, the optical spectra are dominated by molecular lines, limiting the extent to which chemical compositions can be determined owing to blending. At NIR wavelengths there are spectral windows that are relatively free of molecular absorption, where lines from heavy elements are located. Furthermore, the reduced effects of extinction in the NIR compared to the visual range allow us to access more distant stars. However, to fully resolve these spectral features and to properly interpret lower resolution spectra, high-resolution spectroscopy is essential (see Figure 8). Currently, line data for many elements, but especially the post-iron group elements, are severely lacking and those that exist are predominantly the result of theoretical calculations. High resolution and high S/N are needed to explore weak atomic lines of poorly observed elements, and isotopic ratios of molecular lines, which will open a window to nuclear fusion processes in stellar interiors. Another topic that can be investigated with the help of such data are small velocity shifts between high and low excitation lines or asymmetries in the line profiles that hint towards velocity fields in a star's atmosphere. Weak emission features that need to be clearly distinguished from absorption components are promising tools to study circumstellar material (Lebzelter *et al.* 2012).

Technical case

With these goals in mind, Lebzelter *et al.* (2012) recently used CRIRES (Käufl *et al.* 2004) on VLT to obtain 1-5 μm spectra of 13 stars evenly spaced across the HR Diagram at a resolving power estimated to be *R*=80,000-90,000. This was done as a 'filler' program on VLT and required about 200 different grating settings per star since CRIRES is a single-order spectrograph. iSHELL can observe the 1-5 μm in at most

17 settings and possibly as few as 11 settings depending on final choice cross-dispersing gratings. A program of 50 bright stars (K< 3) across the HR diagram could be done in about 20 nights.

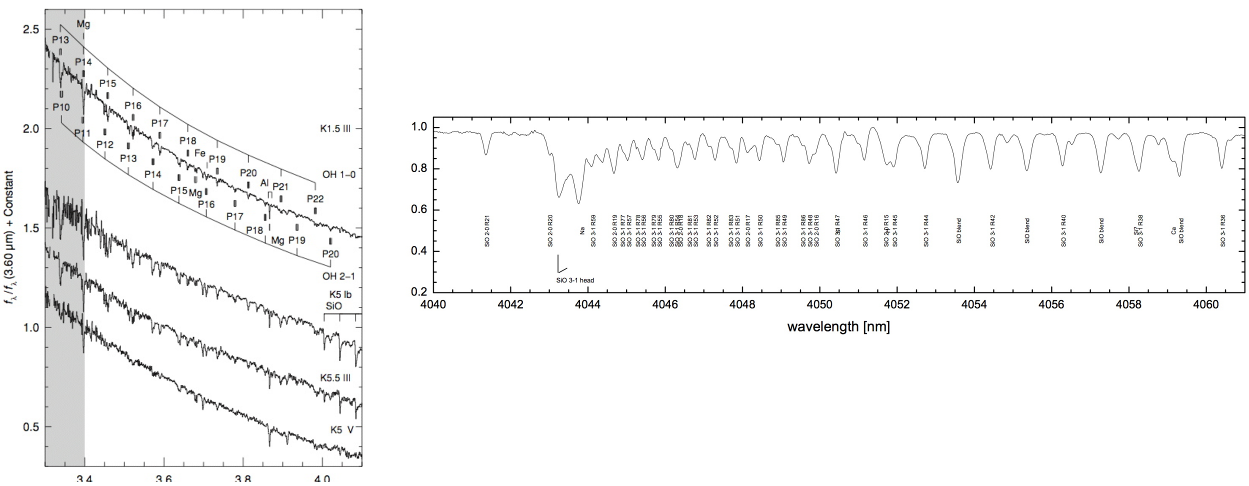

Figure 8. ***(Left)***. Excerpt from the IRTF Spectral Library (R=2500, Rayner *et al*. 2009) showing SiO lines at 4 μm in K dwarf, giant and supergiant stars. ***(Right*).** Detail of the SiO line 4.03-4.06 μm a K supergiant (R=80,000, Lebzelter *et al.* 2012).

Table 2.12 Stellar library science drivers

Parameter	**Requirement**	
	Essential	**Optimum**
Resolving power (R)?	R=50,000	R=100,000
Wavelength coverage?	One shot ≤λ/10 (to minimize grating positions) and sum 1-5 μm	≤λ/5
Target brightness, number of targets?	K≤3, ~50 targets?	
Required S/N	≥100	
Spatial resolution?	Point source	
Slit length?	15″	5″
Rotate slit?	No	
Sky subtraction?	Nod in slit or fit sky along slit	
Standard star?	TBD. Possibly use telluric model.	
Wavelength calibration?	Arcs and telluric features	
Acquisition?	IR imaging	
Guiding?	Yes, spill-over from target in slit or o-a visible guider	
Imaging?	*JHKLM′* photometry	

3. References

Adriano, A. and 12 co-authors 2008. JIRAM, the Image Spectrometer in the near infrared on board the Juno mission to Jupiter. Astrobiology 8, 613-622.

Baines, K. H., T. W. Momary, B. J. Buratti, D. L. Matson, R. M. Nelson, P. Drossart, B. Sicardy, V. Formisano, G. Bellucci, A. Coradini, C. Griffith, R. H. Brown, J. P. Bibring, Y. Langevin, F. Capaccioni, P. Cerroni, R. N. Clark, M. Combes, D. P. Cruikshank, R. Jaumann, T. B. McCord, V. Mennella, P. D. Nicholson, and C. Sotin (2005). The atmospheres of Saturn and Titan in the near-infrared: First results of Cassini/VIMS. Earth, Moon, and Planets 96, 119-147.

Biver, N., Bockelée-Morvan, D., Crovisier, J., Colom, P., Henry, F., et al. 2002 Chemical Composition Diversity Among 24 Comets Observed At Radio Wavelengths. Earth Moon and Planets 90, 323.

Blake, G. A. & Boogert, A. C. A. 2004 High-Resolution 4.7 Micron Keck/NIRSPEC Spectroscopy of the CO Emission from the Disks Surrounding Herbig Ae Stars. ApJ 606, L73.

Blake, C. H., Charbonneau, D., White, R. J., Torres, G., Marley, M.~S., & Saumon, D. 2008, ApJ, 678, L125

Blake, C. H., Charbonneau, D., White, R. J., Marley, M. S., & Saumon, D. 2007, ApJ, 666, 1198

Boden, A. F., Creech-Eakman, M. J. & Queloz, D. 2000 The Visual Orbit and Evolutionary State of 12 Bootis. ApJ 536, 880.

Brittain, S. D., Rettig, T. W., Simon, T., Kulesa, C., DiSanti, M. A., et al. 2003 CO Emission from Disks around AB Aurigae and HD 141569: Implications for Disk Structure and Planet Formation Timescales. ApJ 588, 535.

Brooke, T. Y., Weaver, H. A., Chin, G., Bockelée-Morvan, D., Kim, S. J., & Xu, L.-H. 2003 Spectroscopy of Comet Hale-Bopp in the infrared. Icarus 166, 167.

Butler, R. P., Johnson, J. A., Marcy, G. W., Wright, J. T., Vogt, S. S., & Fischer, D. A. 2006, PASP, 118, 1685

Carr, J. S., Mathieu, R. D. & Najita, J. R. 2001 Evidence for Residual Material in Accretion Disk Gaps: CO Fundamental Emission from the T Tauri Spectroscopic Binary DQ Tauri. ApJ 551, 454.

Carr, J. S., Tokunaga, A. T. & Najita, J. 2004 Hot H2O Emission and Evidence for Turbulence in the Disk of a Young Star. ApJ 603, 213.

Charbonneau, D., Allen, L. E., Megeath, S. T., Torres, G., Alonso, R., et al. 2005 Detection of Thermal Emission from an Extrasolar Planet. ApJ 626, 523.

Covey, K. R., Greene, T. P., Doppmann, G. W. & Lada, C. J. 2005 The Angular Momentum Content and Evolution of Class I and Flat-Spectrum Protostars. Astronomical Journal 129, 2765.

Dello Russo, N. D., Mumma, M. J., DiSanti, M. A. & Magee-Sauer, K. 2002b Production of ethane and water in comet C/1996 B2 Hyakutake. Journal of Geophysical Research (Planets) 107k, 5.

Dello Russo, N., Disanti, M. A., Magee-Sauer, K., Gibb, E. L., Mumma, M. J., et al. 2004 Water production and release in Comet 153P/Ikeya-Zhang (C/2002 C1): accurate rotational temperature retrievals from hot-band lines near 2.9-mum. Icarus 168, 186.

Dello Russo, N., Mumma, M.J., Disanti, M.A., Magee-Sauer, K., Gibb, E.L., Bonev, B.P., McLean, I.S., Xu, L.-H. 2006 A high-resolution infrared spectral survey of Comet C/1999 H1 Lee, Icarus 184, 255.

Deming, D., Seager, S., Richardson, L. J. & Harrington, J. 2005 Infrared radiation from an extrasolar planet. Nature 434, 740.

Deming, Drake; Harrington, Joseph; Seager, Sara; Richardson, L. Jeremy 2006 Strong Infrared Emission from the Extrasolar Planet HD 189733b, ApJ 644, 560.

de Pater, I., M. H. Wong, P. Marcus, S. Luszcz-Cook, M. Adamkovics, A. Conrad, X. Asay- Davis, and C. Go 2010. Persistent rings in and around Jupiter's anticyclones – Observations and theory.

Icarus 210, 742-762.
de Pater, I., M. H. Wong, K. de Kleer, H. B. Hammel, M. Adamkovics, and A. Conrad 2011. Keck adaptive optics images of Jupiter's north polar cap and Northern Red Oval. Icarus 213, 559-563.
Doppmann, G. W. & Jaffe, D. T. 2003 A Spectroscopic Technique for Measuring Stellar Properties of Pre-Main-Sequence Stars. Astronomical Journal 126, 3030.
Doppmann, G. W., Jaffe, D. T. & White, R. J. 2003 Stellar Properties of Pre-Main-Sequence Stars from High-Resolution Near-Infrared Spectra. Astronomical Journal 126, 3043.
Doppmann, G. W., Greene, T. P., Covey, K. R. & Lada, C. J. 2005 The Physical Natures of Class I and Flat-Spectrum Protostellar Photospheres: A Near-Infrared Spectroscopic Study. Astronomical Journal 130, 1145.
Durisen, R. H., Boss, A. P., Mayer, L., Nelson, A. F., Quinn, T., & Rice, W.~K.~M. 2007, Protostars and Planets V, 607
Ershov, O. A., Jaffe, D. T., Marsh, J. P. & Keller, L. D. 2001 Production of high-order micromachined silicon echelles on optically flat substrates. In Proc. SPIE Vol. 4440, p. 301-308, Lithographic and Micromachining Techniques for Optical Component Fabrication, Ernst-Bernhard Kley; Hans-Peter Herzig; Eds., vol. 4440, pp. 301.
Gibb, E. L., Mumma, M. J., dello Russo, N., Disanti, M. A. & Magee-Sauer, K. 2003 Methane in Oort cloud comets. Icarus 165, 391.
Gibb, E L.; Van Brunt, K. A.; Brittain, S. D.; Rettig, T. W. 2007. ApJ, Volume 660, Issue 2, pp. 1572-1579
Graf, U. U., Jaffe, D. T., Kim, E. J., Lacy, J. H., Ling, H., et al. 1994 Fabrication and evaluation of an etched infrared diffraction grating. Applied Optics 33, 96.
Greene, T. P. & Lada, C. J. 2000 High-Resolution Near-Infrared Spectra of Protostars. Astronomical Journal 120, 430.
Greene, T. P. & Lada, C. J. 2002 Spectroscopic Detection of a Stellar-like Photosphere in an Accreting Protostar. Astronomical Journal 124, 2185.
Harrington, J., Hansen, B.M., Luszcz, S.H., Seager, S., Deming, D., Menou, K., Cho, J. Y.-K.; Richardson, L.J. 2006 The Phase-Dependent Infrared Brightness of the Extrasolar Planet υ Andromedae b, Science, 314 623.
Huerta, M., Johns-Krull, C. M., Prato, L., Hartigan, P., & Jaffe, D. T. 2008, ApJ, 678, 472
Jaffe, D. T., Keller, L. D. & Ershov, O. A. 1998 Micromachined silicon diffraction gratings for infrared spectroscopy. In Proc. SPIE Vol. 3354, p. 201-212, Infrared Astronomical Instrumentation, Albert M. Fowler; Ed., vol. 3354, pp. 201.
Johns-Krull, C. M. & Valenti, J. A. 1996 Detection of Strong Magnetic Fields on M Dwarfs. ApJ 459, L95.
Johnson, J. A., et al. 2007, ApJ, 665, 785
Käufl, H. U., Ballester, P., Biereichel, P., et al. 2004, SPIE, 5492, 1218
Kawakita, H., Watanabe, J.-i., Kinoshita, D., Ishiguro, M. & Nakamura, R. 2003 Saturated Hydrocarbons in Comet 153P/Ikeya-Zhang: Ethane, Methane, and Monodeuterio-Methane. ApJ 590, 573.
Larson, H. P., U. Fink, H. A. Smith, and D. S. Davis (1980). The middle-infrared spectrum of Saturn: evidence for phosphine and upper limits to other trace atmospheric constituents. Astrophys. J. 240, 327-337.
Lebzelter, T.; Seifahrt, A.; Uttenthaler, S.; Ramsay, S.; Hartman, H.; Nieva, M.-F.; Przybilla, N.; Smette, A.; Wahlgren, G. M.; Wolff, B.; Hussain, G. A. J.; Käufl, H. U.; Seemann, U. 2012. Astronomy & Astrophysics, Volume 539, id.A109, 25 pp.
Magee-Sauer, K., dello Russo, N., Disanti, M. A., Gibb, E. & Mumma, M. J. 2002 Production of HCN and C2H2 in comet C/2002 C1 Ikeya-Zhang on UT 2002 April 13.8. In ESA SP-500: Asteroids,

Comets, and Meteors: ACM 2002, pp. 549.
Marois, C., Macintosh, B., Barman, T., Zuckerman, B., Song, I., Patience, J., Lafreniere, D., & Doyon, R. 2008, Science, 332 (5906): 1348, arXiv:0811.2606
Mazeh, T., Simon, M., Prato, L., Markus, B., Zucker, S. 2003 The Mass Ratio Distribution in Main-Sequence Spectroscopic Binaries Measured by Infrared Spectroscopy, ApJ 599, 1344.
Miller, S., Aylward, A., Millward, G. 2005 Giant Planet Ionospheres and Thermospheres: The Importance of Ion-Neutral Coupling, Space Science Reviews 116, 319.
Moore, J., Ling, H., Graf, U.U., & Jaffe, D.T. 1992, Microwave and Opt. Tech. Letters 5, 480.
Mumma, M. J., Weissman, P. R. & Stern, S. A. 1993 Comets and the origin of the solar system - Reading the Rosetta Stone. In Protostars and Planets III, pp. 1177.
Mumma, M. J., Dello Russo, N., DiSanti, M. A., Magee-Sauer, K., Novak, R. E., et al. 2001 Organic Composition of C/1999 S4 (LINEAR): A Comet Formed Near Jupiter? Science 292, 1334.
Mumma, M. J., Disanti, M. A., dello Russo, N., Magee-Sauer, K., Gibb, E., et al. 2003 Remote infrared observations of parent volatiles in comets: A window on the early solar system. Advances in Space Research 31, 2563.
Mumma, Michael J., Villanueva, G. L., Bonev, B. P., DiSanti, M. A., Magee-Sauer, K., Salyk, C., Blake, G. A. 2006 The Unusual Organic Volatile Composition of Comet 73P/Schwassmann-Wachmann 3: Is SW3 the Third Member of a Distinct Taxonomic Group? BAAS, DPS mtg. 38, #03.08.
Mumma, Michael J., Villanueva, G. L., Novak, R. E.., Hewagama, T., Bonev, B. P., DiSanti, M. A.., Mandel, A. M., and Smith, M. D. 2009 Strong Release of Methane on Mars in Northern Summer 2003. Science, 323, 1041M
Najita, J., Carr, J. S. & Mathieu, R. D. 2003 Gas in the Terrestrial Planet Region of Disks: CO Fundamental Emission from T Tauri Stars. ApJ 589, 931.
Papaloizou, J. C. B., Nelson, R. P., Kley, W., Masset, F.~S., & Artymowicz, P. 2007, Protostars and Planets V, 655
Prato, L., Simon, M., Mazeh, T., McLean, I. S., Norman, D., et al. 2002a The Smallest Mass Ratio Young Star Spectroscopic Binaries. ApJ 569, 863.
Prato, L., Simon, M., Mazeh, T., Zucker, S. & McLean, I. S. 2002b Component Masses of the Young Spectroscopic Binary UZ Tau E. ApJ 579, L99.
Prato, L., Huerta, M., Johns-Krull, C. M., Mahmud, N., Jaffe, D. T., & Hartigan, P. 2008, ApJ, 687, L103
Rayner, John T.; Cushing, Michael C.; Vacca, William D. 2009. The Astrophysical Journal Supplement, Volume 185, Issue 2, pp. 289-432
Rego, D., Achilleos, N. Stallard, T., Miller, S., Prange, R., et al. 1999 Supersonic winds in Jupiter's Aurorae. Nature 399, 121
Scoville, N.; Kleinmann, S. G.; Hall, D. N. B.; Ridgway, S. T; 1983. Astrophysical Journal, Part 1 (ISSN 0004-637X), vol. 275, Dec. 1, 1983, p. 201-224
Setiawan, J., Weise, P., Henning, T., Launhardt, R., M"uller, A., & Rodmann, J. 2007, ApJ, 660, L145
Shu, F., Najita, J., Ostriker, E., Wilkin, F., Ruden, S., et al. 1994 Magnetocentrifugally driven flows from young stars and disks. 1: A generalized model. ApJ 429, 781.
Simon, M. & Prato, L. 2004 The Double-lined Spectroscopic Binary Haro 1-14c. ApJ 613, L69.
Simon-Miller, A. A., B. Conrath, P. J. Gierasch, and R. F. Beebe 2000. A detection of water ice on Jupiter with Voyager IRIS. Icarus 145, 454-461.

Snellen, Ignas A. G.; de Kok, Remco J.; de Mooij, Ernst J. W.; Albrecht, Simon; 2010. Nature, Volume 465, Issue 7301, pp. 1049-1051.
Stallard, T. S., Miller, S., Trafton, L. M., Geballe, T. R. & Joseph, R. D. 2004 Ion winds in Saturn's southern auroral/polar region. Icarus 167, 204.

Steffen, A. T., Mathieu, R. D., Lattanzi, M. G., Latham, D. W., Mazeh, T., et al. 2001 A Dynamical Mass Constraint for Pre-Main-Sequence Evolutionary Tracks: The Binary NTT 045251+3016. Astronomical Journal 122, 997.

Tsiganis, K.; Gomes, R.; Morbidelli, A.; Levison, H. F. 2005 Origin of the orbital architecture of the giant planets of the Solar System, Nature 435, 459.

Villanueva, G.L., Bonev, B.P., Mumma, M.J., Magee-Sauer, K., DiSanti, M.A., Salyk, C., Blake, G.A. 2006 The Volatile Composition of the Split Ecliptic comet 73P/Schwassmann-Wachmann 3: A Comparison of Fragments C and B, ApJ 650, L87.

Weaver, H. A., Chin, G., Bockelée-Morvan, D., Crovisier, J., Brooke, T. Y., et al. 1999 An Infrared Investigation of Volatiles in Comet 21P/Giacobini-Zinner. Icarus 142, 482.

Weidenschilling, S. J., and J. S. Lewis 1973. Atmospheric and cloud structures of the Jovian planets. Icarus 20, 465-476.

White, R.J.; Hillnebrand, L.A; 2005. The Astrophysical Journal, Volume 616, Issue 2, pp. 998-1032.

White, R. J.; Greene, T. P.; Doppmann, G. W.; Covey, K. R.; Hillenbrand, L.A.; 2007. Protostars and Planets V, B. Reipurth, D. Jewitt, and K. Keil (eds.), University of Arizona Press, Tucson, 951 pp., p.117-132

Wong, M.H., J. Lunine, S.K. Atreya, T. Johnson, P.R. Mahaffy, T.C. Owen, and T. Encrenaz 2008. Oxygen and other volatiles in the giant planets and their satellites, in Reviews in Mineralogy and Geochemistry Vol. 68: Oxygen in the Solar System (G.J. MacPherson et al., eds.), Mineralogical Society of America